Energy 75 (2014) 116–126

Contents lists available at ScienceDirect

Energy

journal homepage: www.elsevier.com/locate/energy

Experimental study on the influence of oxygen content in the combustion air on the combustion characteristics

Petr Bělohradský*, Pavel Skryja, Igor Hudák

Institute of Process and Environmental Engineering, Faculty of Mechanical Engineering, Brno University of Technology, Technická 2, Brno 61669, Czech Republic

ARTICLE INFO

Article history:
Received 20 December 2013
Received in revised form
2 April 2014
Accepted 9 April 2014
Available online 6 May 2014

Keywords:
Oxygen-enhanced combustion
Staged combustion
Nitrogen oxides
Heat flux
Flame pattern

ABSTRACT

This study was focused on the experimental investigation of the very promising combustion technology called as the oxygen-enhanced combustion (OEC), which uses the oxidant containing higher proportion of oxygen than in the atmospheric air, i.e. more than 21%. The work investigated and compared the characteristics of two OEC methods, namely the premix enrichment and air-oxy/fuel combustion, when the overall oxygen concentration was varied from 21% to 46%. The combustion tests were performed with the experimental two-gas-staged burner of low-NO_x type at the burner thermal input of 750 kW for two combustion regimes – one-staged and two-staged combustion. The oxygen concentration in the flue gas was maintained in the neighborhood of 3% vol. (on dry basis). The aim of tests was to assess the impact of the oxidant composition, type of OEC method and fuel-staging on the characteristic combustion parameters in detail. The investigated parameters included the concentration of nitrogen oxides (NO_x) in the flue gas, flue gas temperature, heat flux to the combustion chamber wall, and lastly the stability, shape and dimensions of flame. It was observed that NO_x emission is significantly lower when the air-oxy/fuel method is used compared to the premix enrichment method. Moreover, when the fuel was staged, NO_x emission was below 120 mg/Nm^3 at all investigated oxygen flow rates. Increasing oxygen concentration resulted in higher heating intensity due to higher concentrations of CO_2 and H_2O. The available heat at 46% O_2 was higher by 20% compared with that at 21% O_2.

1. Introduction

Most industrial heating processes require substantial amounts of energy, which is commonly generated by combusting hydrocarbon fuels such as natural gas or heating oil [1]. The majority of industrial combustion processes use the atmospheric air as the oxidant, which consists of approximately 21% O_2 and 79% N_2 by volume. However, only oxygen is needed in the combustion reaction and nitrogen in air acts as a ballast that has to be heated up and carries the energy of the combustion process out with the hot flue gas, which decreases the thermal efficiency of the combustion process. Many of high-temperature processes use an oxidant containing higher proportion of oxygen than in the atmospheric air. This type of combustion is referred to as oxygen-enhanced combustion (OEC) and has many benefits including increased processing rates, higher heat transfer efficiency, improved flame characteristics, reduced equipment cost and last but not least improved product quality [2]. However, there are also potential problems associated with the use of OEC if the system is not properly designed, e.g. refractory or burner damage, non-uniform heating and/or increased pollutant emissions.

Combustion processes are commonly enhanced by oxygen in four primary ways [2]: (1) adding O_2 into the incoming airstream (referred to as low-level O_2 enrichment or premix enrichment), (2) injecting O_2 into an air/fuel flame (referred to as O_2 lancing), (3) separately provided combustion air and O_2 to the burner (referred to as air-oxy/fuel combustion), (4) replacing the combustion air with high-purity O_2 (referred to as oxy/fuel combustion) that is known as a promising technology for capturing of CO_2 from the flue gas [3–5].

When the low-level oxygen enrichment (21–30% O_2) is applied to the existing combustion equipment minor burner modifications need to be made to permit operation at slightly higher O_2 concentrations. It is especially used in cases when the production rate in the heating process can be significantly increased even with only relatively small amounts of oxygen enrichment. In case the

* Corresponding author. Tel.: +420 541 144 959.
E-mail address: belohradsky@fme.vutbr.cz (P. Bělohradský).

http://dx.doi.org/10.1016/j.energy.2014.04.026
0360-5442/

Nomenclature

$M(NO)$	Molar mass of nitric oxide NO [g/mol]
$M(NO_2)$	Molar mass of nitrogen dioxide NO_2 [g/mol]
V_m	Molar volume of ideal gas (=22.414 l/mol)
$\dot{Q}_i$	Heat transfer rate to the wall of i-th chamber's section [W]
$\dot{m}_i$	Mass flow rate of cooling water through i-th chamber's section [kg/s]
Δt_i	Temperature difference between outlet and inlet temperature of cooling water [°C]
$\dot{q}_i$	Heat flux to the wall of i-th chamber's section [kW/m^2]
$\dot{V}_i$	Volumetric flow rate of cooling water through i-th chamber's section [m^3/h]
$c_{p,i}$	Specific heat capacity of cooling water in i-th chamber's section [J/kg K]
ρ_i	Density of cooling water in i-th chamber's section [kg/m^3]
$t_{OUT,i}$	Outlet temperature of cooling water out of i-th chamber's section [°C]
t_{IN}	Inlet temperature of cooling water in chamber [°C]
A_i	Flame-facing area of i-th chamber's section [m^2]
L_i	Length of i-th chamber's section [m]
σ_{NO_X}	Standard deviation of calculated NO_X [mg/Nm^3]
σ_{NO}	Standard deviation of measured NO converted to NO_2 equivalent and expressed in [mg/Nm^3]
σ_{NO_2}	Standard deviation of measured NO_2 expressed in [mg/Nm^3]
$\sigma_{\dot{q}_i}$	Standard deviation of calculated heat flux to the wall of i-th chamber' section [kW/m^2]
$\sigma_{\dot{V}_i}$	Standard deviation of water flow rate through i-th chamber's section [m^3/h]
$\sigma_{t_{OUT,i}}$	Standard deviation of outlet temperature of cooling water out of i-th chamber's section [°C]
$\sigma_{t_{IN}}$	Standard deviation of inlet temperature of cooling water in chamber [°C]

Acronyms

OEC	Oxygen-enhanced combustion
PE	Premix enrichment
AO	Air-oxy/fuel combustion

combustion system is operated in intermediate (30–90% O_2) or high-level (>90% O_2) oxygen enrichment regime the existing air/fuel burners have to be replaced by burners specifically designed to use the higher levels of O_2.

Economically, the method of low-level oxygen enrichment can save the cost for retrofits of existing burners. However, the characteristics of low-level oxygen enrichment in an air/fuel combustion system have been studied rarely thus far. The group of Wu et al. [6] studied the influence of 21–30% oxygen concentration on the heating rate, emissions, temperature distributions and fuel consumption in the heating and furnace-temperature fixing tests. They found in the heating tests that compared to the air with 21% O_2, the time elapsed for heating to 1200 °C was only 46% for air with 30% O_2. As for the species concentrations the NO_x emission was increased by 4.4 times and CO_2 increased almost linearly when the oxygen concentration was increased from 21% to 30%. The furnace-temperature fixing tests showed that the fuel consumption at 30% O_2 was reduced by 26%, compared with that at 21% O_2. Merlo et al. [7] studied the oxygen enrichment effects on the stability of methane-air non-premixed swirling flame, and on the pollutant emissions like CO, CO_2 and NO_x. They reported that oxygen enrichment promotes higher CO conversion into CO_2, NO_x emissions increase strongly with oxygen addition mainly due to the increase of the flame temperature, and the flame stability is enhanced with oxygen addition even for low oxygen enrichment rates. Daood et al. [8] studied the influence of different oxygen concentrations and staging levels on NO reduction and carbon burnouts during the coal air-staged combustion. The experiments revealed that oxygen-enriched air-staged combustion at the 31% level of staging resulted in approximately 7% and 35% NO reduction for 28% and 35% overall oxygen concentration, respectively. Moreover the oxygen enrichment improved the carbon burnouts. Tan et al. [9] used down fired vertical combustor to study oxygen-enhanced and O_2/CO_2 combustion. They concluded that very high levels of NO_x emissions are achieved due to higher flame temperatures that are related to higher oxygen concentration in the feed air used in the oxygen-enhanced combustion. However, in O_2/CO_2 combustion the NO_x formation is suppressed because N_2 is not present in the feed air, only air leakage at the fan contributed to the formation of NO_x in small concentrations. The impact of OEC was also study in large steam boilers [10]. The use of OEC in boilers leads to the increase of the flue gas temperature and in this way, the heat transfer surfaces can be reduced due to the higher mean log temperature differences within the heat exchangers of the boiler, and the boiler's efficiency can be increased by 2% up to 5% at the same time.

A few research groups have investigated the membrane separation as an air-enrichment technique [11,12]. For instance, Qiu and Hayden [11] explored OEC of natural gas in porous ceramic radiant burners, when the oxygen enriched air was produced passively using polymer membranes. The oxygen concentration was varied between 21% and 28%. The experimental results showed that the potential saving in natural gas consumption was about 22% when oxygen concentration was increased to 28%.

A few studies of oxygen-enhanced combustion have been also carried out in the field of flameless combustion, e.g. by Sánchez et al. [13] who investigated the effect of oxygen enrichment from 21% to 35% vol. on the performance of flameless combustion furnace equipped with a regenerative burner. The results showed that for all oxygen enrichment rates it was possible to obtain no luminous effect, wide reaction zone and uniform temperature profile, which are typical features of flameless combustion phenomena. NO_x emissions were below 5 ppm and the global efficiency increased almost 5% for an oxygen enriched level of 30%.

This work is a follow-up to the experimental study of the influence of geometry of the gas-staged burner from the view of NO_x formation [14]. The present work investigated and compared the characteristics of two OEC methods, namely of the premix enrichment (further in the text denoted as PE) and air-oxy/fuel combustion (denoted as AO). The study was aimed at the studying the influence of 21–46% oxygen concentration on the NO_x emission, flue gas temperature, distribution of heat extracted from the hot flue gas to the wall of the combustion chamber, and the flame pattern including stability, shape and dimensions. The combustion tests of PE and AO were carried out at the burner thermal input of 750 kW for two combustion regimes – one-staged combustion and two-staged combustion. The target oxygen concentration in dry flue gas was 3% vol.

2. Experimental setup

2.1. Testing facility

The combustion tests were carried out at the large-scale burners testing facility shown in Fig. 1. The facility enables testing of gaseous fuel burners, liquid fuel burners and/or dual fuel burners up to the thermal input of 1800 kW. The detailed description of the testing facility can be also found in Ref. [15].

The key apparatus of the facility is the two-shell horizontal water-cooled combustion chamber with the inner diameter of 1 m and the length of 4 m. The front side and the rear side of the chamber are insulated with the high temperature fibrous lining with the thickness of 100 mm. The cooling shell of the combustion chamber is divided into seven individual sections with independent supply of cooling water. Six sections have the length of 0.5 m; the last seventh section has the length of 1 m. Each section is equipped with sensors for the measurement of flow rate, inlet and outlet temperature of cooling water. This unique construction enables to partially simulate conditions similar to the ones in fired process heaters and to evaluate the heat flux rate from the hot flue gas to the combustion chamber shell lengthwise the flame. The technical parameters of the sensors of the water cooling system are summarized in Table A.1 in Appendix A.

The combustion chamber is equipped with eight inspection windows along the cylindrical part. There are further two inspection windows on the rear side opposite the burner which allow observing of the flame on the burner.

Flue gas is exhausted from the combustion chamber through the flue gas stack with the inner diameter of 0.5 m. There are three measurements and sampling spots for measuring pressure in the combustion chamber, flue gas temperature and flue gas composition. The flue gas analysis and flue gas temperature measurement are provided by the flue gas analyzer TESTO 350-XL analyzer. The analysis box is equipped with the electrochemical sensors for real time measurement of O_2, CO, CO_2, NO and NO_2 concentrations in dry flue gas. The flue gas temperature is measured using the thermocouple of type K. The measuring ranges and accuracies of measuring instrumentation are summarized in Table A.2 in Appendix A.

2.2. Burner

The two-gas-staged power burner with the maximal thermal input of 1500 kW fired by natural gas was used for tests. The 3D model of the burner is shown in Fig. 2. Both the diameter of burner body, through which the combustion air is fed into the burner, and the inner diameter of burner quarl is 300 mm. The gas inlet consists of twelve primary nozzles and eight secondary nozzles. The primary nozzles are drilled in the primary nozzle head and are aligned in two circular sets. There are four nozzles with the diameter of 3.0 mm in the first set and eight nozzles with the diameter of 2.6 mm in the second set. The maximum thermal input of the primary stage can be regulated by the exchangeable primary gas throttle of different diameters placed before the inlet to the primary stage of the burner. During the tests, when staged combustion was used, the ratio primary/total fuel flow rate was set to 0.28.

The secondary gas inlet is provided by four nozzle heads with the pitch angle of head 30°. Each head has two nozzles with the diameter of 3.3 mm. The burner is constructed so that it is possible to change the position of secondary nozzle heads toward the burner tile in tangential and radial direction. In the reference tangential position the nozzles are oriented directly toward the burner axis. The orientation can be changed both clockwise (i.e. in the direction of flame (air) swirl motion – positive angle) and counter clockwise (i.e. negative angle). In the reference radial distance the distance of nozzle heads from the burner axis is 180 mm and can be extended by 50 mm. During the tests, when staged combustion regime was used, the secondary nozzle heads were turned by 20° in the direction of flame motion and their radial distance was set to the maximum, i.e. 230 mm from the burner axis.

The burner is equipped with the so-called flame holder that has the form of swirl generator. The swirl generator consists of eight pitched blades and is mounted to the central burner pipe. The swirl generator used in tests was characterized with the diameter of 240 mm and pitch angle of swirl generator's blades of 35°. Flame

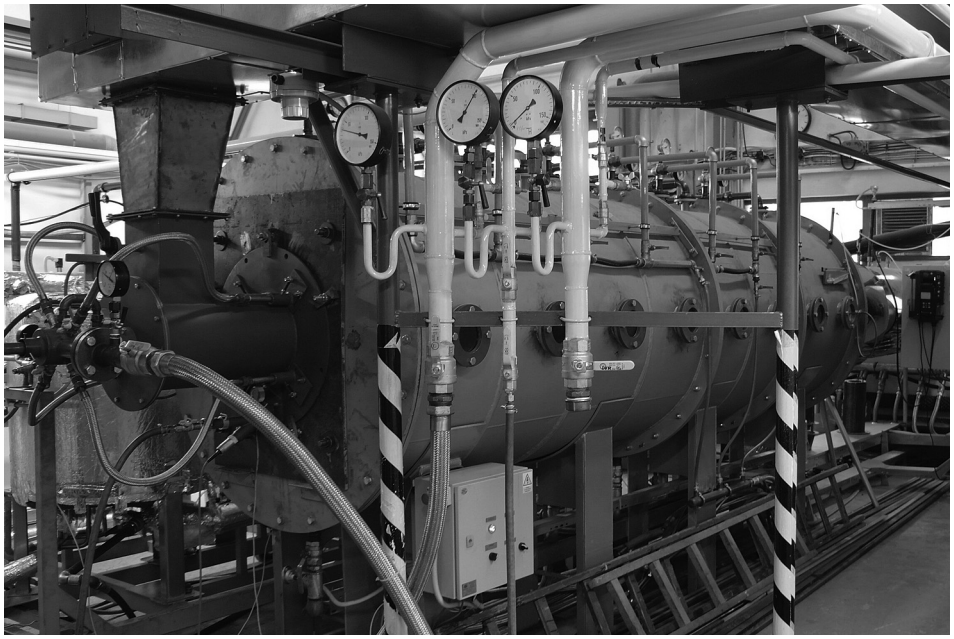

Fig. 1. The burners testing facility.

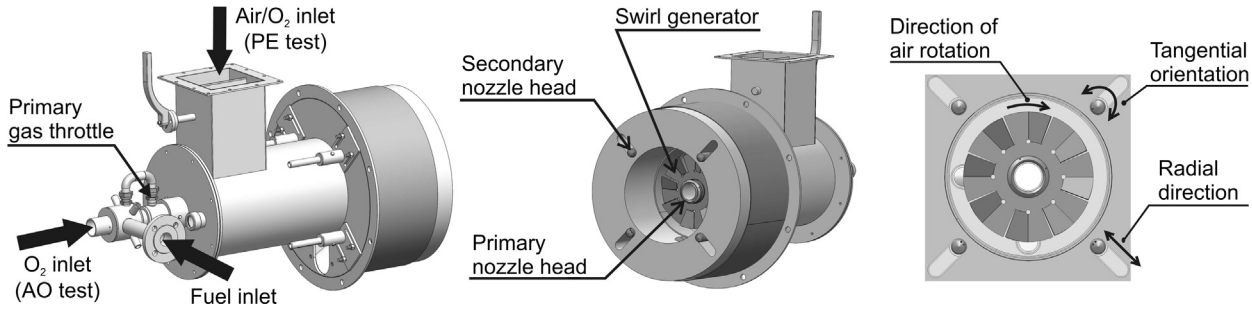

Fig. 2. The 3D model of experimental two-gas-staged burner.

ignition is performed with a gaseous premixed natural–draught ignition burner with the thermal input of 18 kW.

2.3. Oxygen supply

The high purity oxygen used for tests was stored in the cryogenic vessel under the pressure of 20 MPa. Before the oxygen was mixed in the air or injected in the combustion chamber, the oxygen passed through the evaporator where its phase state was changed from liquid to gaseous.

When the PE tests were carried out, the high-purity oxygen was injected into the incoming combustion airstream through the diffuser to ensure adequate mixing. The schematic layout of the tip of the diffuser is shown in Fig. A.1 in Appendix A. The diffuser was inserted in the air supply duct before entering the burner. It was designed for the maximal oxygen flow rate of 160 Nm^3/h (at normal conditions 0 °C, 101.325 kPa). Totally 13 holes with the diameter of 2.1 mm are drilled in the body of the diffuser when 12 holes are aligned in six rows, each row with two holes (even rows are positioned at angle 90° toward odd rows) and one hole is located in the closed end of the diffuser.

When the AO tests were carried out, the high-purity oxygen was injected directly into the flame through the nozzle head that was inserted through the center burner pipe. The schematic layout of the tip of the nozzle head is shown in Fig. A.2 in Appendix A. The balance of the oxygen that is necessary for complete combustion was introduced to the burner via the atmospheric air. There are totally seven nozzles with the diameter of 2.7 mm drilled in the head when six nozzles are arranged symmetrically in a ring pattern around the tip of the head and the last nozzle is located at the tip of the head. The nozzle head was designed for the maximal flow rate of oxygen 120 Nm^3/h.

2.4. Plan of combustion tests

The experimental matrix is presented in Table 1. All tests were carried out at the burner thermal input of 750 kW. The target oxygen concentration in the flue gas was 3% by volume (on a dry basis) for all tests.

The investigation was aimed at studying the influence of 21–46% oxygen concentration on the NO_x emission, flue gas temperature, heat flux distribution to the wall of combustion chamber lengthwise the flame, and the flame pattern. As for the PE tests, the O_2 concentration between 21 and 46% matches directly the O_2 concentration in the incoming combustion air. On the other hand, in the AO tests the oxygen was not mixed with the combustion air in the air supply duct and hence the oxygen concentration in the incoming air was always 21%. Thus the term 21–46% oxygen concentration here expresses the overall oxygen concentration as if both airstream and oxygen stream (injected directly in the flame) are mixed.

Two tests were of interest here. In the first test, denoted as TEST A, the quality and the flame characteristics were explored. This included NO_x and CO emissions, flue gas temperature at the outlet of chamber as well as the burning stability and visual character (particularly length and diameter) of oxygen-enhanced flames. Before the start of experiments the combustion chamber was set into steady thermodynamic state. The condition necessary for beginning of data collection was in accordance with the burner testing standards, i.e. the flue gas temperature must not exceed the

Table 1
Experimental matrix (● indicates that the test was carried out for the relevant oxygen flow rate).

Trial – combustion regime	Flow rate of high-purity O_2 [Nm^3/h]/O_2 concentration in the air [%]									
	0/21	5/21.5	10/22	20/23.1	30/24.3	40/25.6	60/29	80/33	100/38	120/46
TEST A										
Premix enrichment										
PE one-staged	●	●	●	●	●	●	●	●	–	–
PE two-staged	●	●	●	●	●	●	●	●	●	●
Air-oxy/fuel										
AO one-staged	●	●	●	●	●	●	●	●	●	–
AO two-staged	●	●	●	●	●	●	●	●	●	–
TEST B										
Premix enrichment										
PE one-staged	●	–	–	–	–	●	–	●	–	–
PE two-staged	●	–	–	–	–	●	–	●	–	●
Air-oxy/fuel										
AO one-staged	●	–	–	–	–	●	–	●	–	–
AO two-staged	●	–	–	–	–	●	–	●	–	–

interval of 10 °C within 30 min. After reaching the state of steadiness the data was collected every minute for time period of 5 min.

The second test, denoted as TEST B, was focused on the evaluation and comparison of local wall heat fluxes into all sections of the combustion chamber. Unlike the TEST A this test was carried out only for selected oxygen flow rates (0, 40, 80, and 120 Nm^3/h). The data collection started after the combustion chamber was set into steady thermodynamic state. This state was considered steady if both flue gas temperature (maximal allowed change within 30 min is 10 °C) and the values of local wall heat fluxes (continuously evaluated) are steady. The data were collected at 2 min intervals for time period of 30 min.

3. Results and discussion

In this section, the effects of OEC methods, oxygen concentration and combustion regimes on the combustion characteristics including NO_x emission, flue gas temperature, heat flux distribution and flame pattern, are described. The measured data related to the TEST A and TEST B is summarized in Table B.1 and Table B.2, respectively, included in Appendix B.

3.1. NO_x emission

Fig. 3 shows the concentrations of NO_x [mg/Nm^3] (at normal conditions 0 °C, 101.325 kPa) as a function of oxygen concentration. The concentration of NO_x [mg/Nm^3] was calculated from the measured concentrations of NO [ppm] and NO_2 [ppm] using the following conversion equation Eq. (1):

$$NO_x\left[mg/Nm^3\right] = \underbrace{\underbrace{\frac{M(NO)}{V_m}}_{=NO[mg/Nm^3]} \cdot \frac{M(NO_2)}{M(NO)} \cdot NO[ppm]}_{=NO\text{ converted to the equivalent value of }NO_2} + \underbrace{\frac{M(NO_2)}{V_m}}_{=NO_2[mg/Nm^3]} \cdot NO_2[ppm], \quad (1)$$

where $M(NO)$ is the molar mass of nitric oxide NO (=30.01 g/mol), $M(NO_2)$ is the molar mass of nitrogen dioxide NO_2 (=46.06 g/mol), V_m is the molar volume (=22.414 l/mol), NO [ppm] and NO_2 [ppm] are the measured concentrations of NO and NO_2 in the units [ppm]. The major proportion of NO_x produced during the combustion was thermal NO_x, which was directly associated with higher flame temperature peaks due to higher O_2 concentration [2,16].

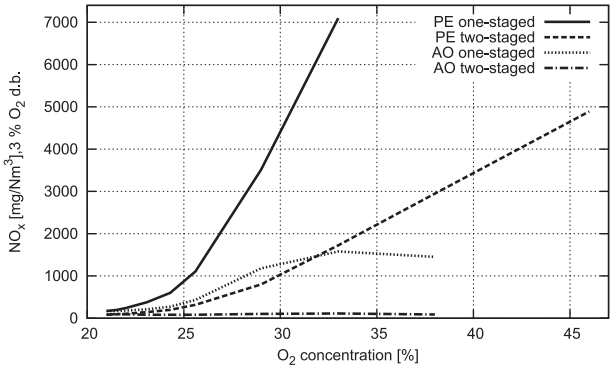

Fig. 3. Effect of oxygen concentration on the NO_x emission.

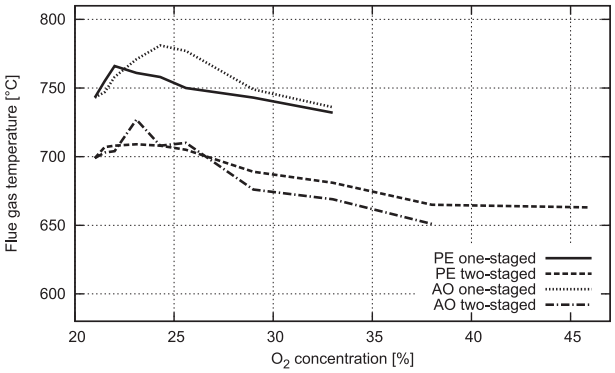

Fig. 4. Effect of oxygen concentration on the flue gas temperature.

As for the PE tests, it can be seen that NO_x showed approximately exponential dependence on the in-flame temperature both for one-staged and two-staged regime. Due to this, even a minor variation in temperature accelerated NO_x formation. When the PE one-staged combustion regime was used, the NO_x emission increased sharply from 170 mg/Nm^3 to 7100 mg/Nm^3 as the O_2 concentration in the combustion air increased from 21% to 33%. Further O_2 enrichment was not possible for this regime for two reasons. First, the measured values of NO_x were out of the measuring range of the analyzer. Second, the swirl generator's blades and burner quarl began to glow due to very high temperature at the burner tile and due to the low flow rate of combustion air that also plays a role of cooler of the burner body.

However, when the PE two-staged combustion regime was used as the NO_x reducing technique, the increase in NO_x formation was not so steep compared to the PE one-staged combustion regime since the reaction of fuel with oxygen was staged. It rose gradually from 82 mg/Nm^3 to 4900 mg/Nm^3 as O_2 concentration increased from 21% to 46%. Moreover, the NO_x concentration was less than 200 mg/Nm^3 (which is the currently valid NO_x emission limit for stationary sources with the thermal input in the range between 0.3 and 50 MW in the Czech Republic) as long as O_2 concentration was less than 25%. Additionally the NO_x reached the value only 1700 mg/Nm^3 at 33% O_2, which is by four times less than obtained in the PE one-staged tests at the same O_2 concentration.

As for the AO tests, the NO_x emission did not increase so dramatically as the O_2 concentration was enhanced compared to the PE tests. The maximum reachable operating flow rate of oxygen in AO tests was 100 Nm^3/h. The higher oxygen flow rate was not possible because the decreasing air flow rate through the burner body caused that the air velocity exiting the burner was lower than the flame speed and flame started to flashback inside the burner.

When the AO one-staged combustion tests were carried out, the NO_x emission increased gradually to 1500 mg/Nm^3 as the

flow rate of injected oxygen increased from 0 Nm^3/h to 80 Nm^3/h (corresponding to the overall oxygen concentration 21–33%), as shown in Fig. 3. It was observed that further increase of O_2 flow rate slightly reduces NO_x. The reason is that the major portion of the fuel is combusted in the flame core into which the high-purity oxygen is injected. Hence the flame core is very rich in the oxygen and poor in the nitrogen which in turn results in very low NO_x, although the flame temperature peaks are very high. The balance of the fuel is combusted with the air (containing reduced amount of N_2) downstream of that main combustion zone at low temperatures that are not favorable for thermal NO formation. It can be assumed that further increasing of O_2 concentration will lower NO_x because less N_2 is available to form NO_x.

The excellent results were obtained when the fuel staging was utilized together with the air-oxy/fuel combustion method. The value of NO_x concentration was fluctuating around the value of 90 mg/Nm^3 and the maximum value reached only 110 mg/Nm^3 at the oxygen flow rate 80 Nm^3/h (corresponding to 33% O_2). The reason was that some of the fuel was directed into the primary combustion zone while the balance of fuel was directed into the secondary zone. This made the primary zone fuel lean, which is less conducive to NO_x formation compared to one-staged combustion [6]. The excess O_2 from the primary zone was then used to combust the secondary fuel. The peak flame temperature was much lower in the fuel staged case because the combustion is staged over some distance. Consequently, the lower temperatures contributed to reduce the NO_x emission. Further increase of O_2 concentration had the same effect as in the AO one-staged tests, i.e. the NO_x reduction.

Summing up, the NO_x emission in the flue gas increased with increasing oxygen concentration in the combustion air when PE OEC method was tested. These results comply with the results acquired with Wu et al. [6] as well as with Persis et al. [17] and Abdelaal et al. [18]. On the other hand, the increase of NO_x was observed significantly steeper than by Merlo et al. [7]. Moreover,

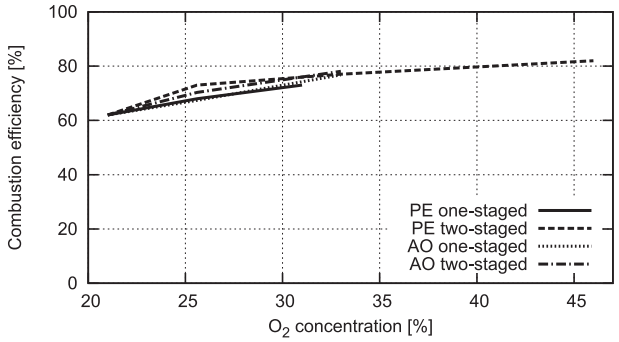

Fig. 6. Effect of oxygen concentration on the combustion efficiency.

Merlo et al. [7] observed very high CO emission at very low O_2 enrichment levels, however, CO emission was observed to be lower than 5 ppm for all O_2 concentrations and all combustion regimes in our tests. As for the AO OEC method, the NO_x concentration was much less than that in PE tests.

3.2. Flue gas temperature

Fig. 4 presents the variation of flue gas temperature at different oxygen concentrations. The graph shows that the flue gas temperature slightly increased as O_2 concentration increased to 23–24%. However, further increase of O_2 concentration caused the moderate decrease in the flue gas temperature. The possible reason was that the flue gas temperature was affected by decreasing concentration of N_2, which absorbs heat and carries energy out with the flue gas. The higher the O_2 concentration in the oxidizer, the less N_2 is introduced in the combustion process and the more flue gas temperature is reduced. This effect is associated with increasing radiant heat flux from the hot flue gas to the combustion

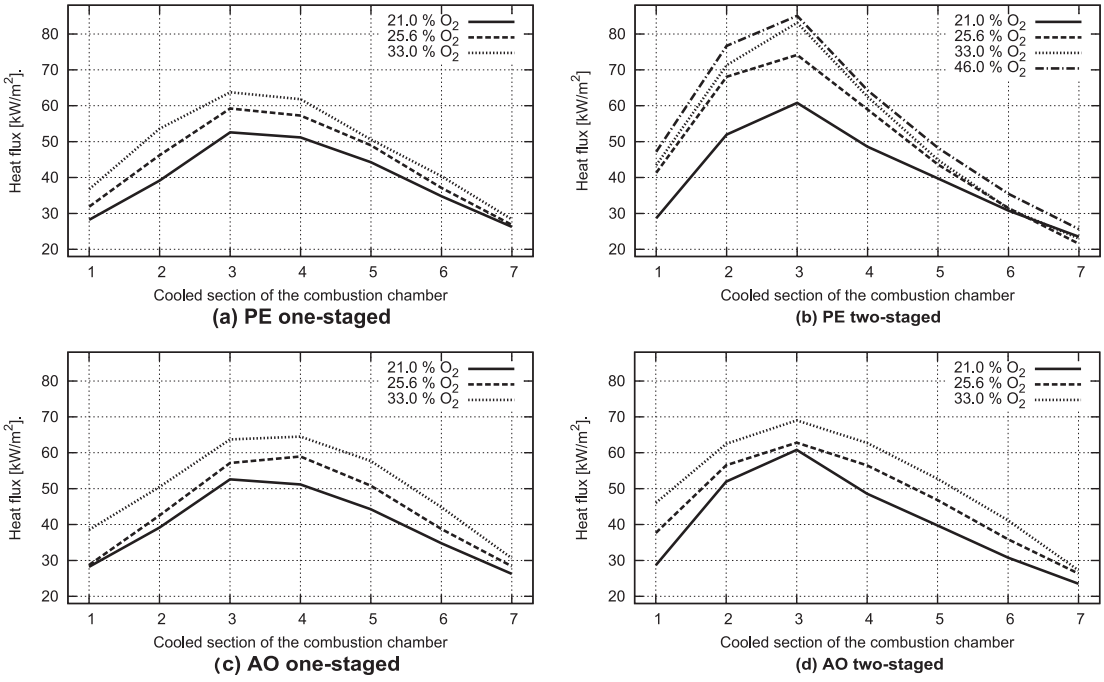

Fig. 5. Heat flux distributions lengthwise the chamber at different oxygen concentrations.

chamber's wall (see Fig. 5 in Section 3.4) and increasing combustion efficiency (see Fig. 6 in section 3.5).

3.3. Flame pattern

The produced oxygen-enhanced flames were observed stable and sharp during all combustion tests. The air/fuel flames were characterized with the blue flame core and the yellow-red envelope. On the other hand, the core of OEC flames became yellower as the O_2 concentration increased. Generally, the produced OEC flames were more luminous compared with the air/fuel flame. Moreover, the flame emissivity is higher, too. This is due to higher concentrations of CO_2 and H_2O, which are the gases that radiate in a flame (there is no radiation from N_2 in the flame).

The dimensions of the visible part of flame including length and diameter were determined based on the subjective observation of the flame by the operator. The observations were carried out through the inspection windows. The flame length was measured from the front of the combustion chamber where the burner is mounted. The flame diameter was then estimated based on the visual comparison of the flame diameter toward the outer diameter of the burner quarl (600 mm) and the inner diameter of the combustion chamber (1 m).

It was observed during the PE tests that the enrichment of oxygen into the combustion airstream lengthened the flame approximately by 25% (from 2.25 m to 3.0 m) as O_2 concentration was increased up to 35%. However, this is in contradiction with Baukal [2] who states that the premix enrichment of oxygen into the combustion airstream shortens the flame length. The plausible explanation for this is that the required amount of the combustion air as well as the exit velocity of enriched-air decrease while O_2 concentration increases, which results in lower mixing intensity of fuel with air. Consequently, the fuel requires for the burnout longer time which results in the flame extension. The diameter was observed in the ranges of 0.5–0.6 m and 0.9–1 m, when the PE one-staged tests and the PE two-staged tests were performed, respectively.

As for the AO one staged tests, it was observed that the flame length was also increased by approximately 25% (from 2.3 m to 3.0 m) as the O_2 concentration was increased. On the other hand, the length of AO two-staged flame was lengthened slightly from 2.2 m to 2.5 m as the O_2 concentration increased from 21% to 35%. Further increase of O_2 concentration, however, caused that the flame was shortened by about 0.3 m. As for the diameter, it was observed in the range of 0.4–0.6 m and of 0.8–1.0 m when the AO one-staged tests and the AO two-staged tests were performed, respectively.

3.4. Heat flux distribution

The burners testing facility utilizes the measurement based on the heat absorbed by the cooling water in each chamber's section. The flame-facing area of the first chamber's section is reduced due to the insulation of the front side of the chamber. Thus the length of the first section is 0.4 m (not 0.5 m) and the flame-facing area is 1.26 m^2. Similarly, the length of the seventh chamber's section is also shortened for the insulation of the rear side of the chamber and hence its length is 0.9 m (not 1 m) and the flame-facing area is 2.83 m^2. The length of sections 2–6 is 0.5 m and the flame-facing area is 1.57 m^2. Since the sections of the combustion chamber represent the calorimetric cells [19], the heat transfer rate in the i-th section can be determined based on the measured volumetric flow rate of the cooling water, inlet water temperature in the section and outlet water temperature out of the section using the balance equation Eq. (2):

$$\dot{Q}_i = \dot{m}_i \cdot c_{p,i} \cdot \Delta t_i \quad \text{for } i = 1, 2, \ldots, 7 \tag{2}$$

where $\dot{Q}_i$ is the heat transfer rate [W], $\dot{m}_i$ is the mass flow rate of the cooling water [kg/s], $c_{p,i}$ is the specific heat capacity [J/kg K], and Δt_i is the temperature difference [°C]. Eq. (2) can be modified for the calculation of the heat flux [kW/m^2] as follows:

$$\dot{q}_i = \frac{1}{1000} \cdot \dot{m}_i \cdot \rho_i \cdot c_{p,i} \cdot (t_{\mathrm{OUT},i} - t_{\mathrm{IN}}) / A_i \quad \text{for } i = 1, 2, \ldots, 7 \tag{3}$$

$$\dot{q}_i = \frac{1}{1000} \cdot \frac{\dot{V}_i}{3600} \cdot \rho_i \cdot c_{p,i} \cdot (t_{\mathrm{OUT},i} - t_{\mathrm{IN}}) / \pi \cdot L_i \quad \text{for } i = 1, 2, \ldots, 7 \tag{4}$$

The water density and specific heat capacity were assumed to be constant in the whole volume of each section and were calculated using the approximation formulas Eqs. (5) and (6) [20], where $\widehat{t}_i = t_{\mathrm{IN}} + t_{\mathrm{OUT},i}$:

$$\rho_i = 1006 - 0.26 \cdot \frac{\widehat{t}_i}{2} - 0.0022 \cdot \left(\frac{\widehat{t}_i}{2}\right)^2 \quad \text{for } i = 1, 2, \ldots, 7 \tag{5}$$

$$c_{p,i} = 4210 - 1.363 \cdot \frac{\widehat{t}_i}{2} + 0.014 \cdot \left(\frac{\widehat{t}_i}{2}\right)^2 \quad \text{for } i = 1, 2, \ldots, 7 \tag{6}$$

The measured heat flux profiles for the TEST B are presented and compared in Fig. 5. As it is evident from the figure, the obtained trend curves of heat flux are characterized with very similar shape for all investigated O_2 concentrations/flow rates and for all combustion regimes. The curves are simply shifted upwards and reach its maximum in the third section for all trials. It can be seen that with increasing O_2 concentration more heat is released from the hot flue gas to the walls of chamber's sections because less energy is wasted in heating up N_2, and the radiative heat transfer is enhanced due to higher concentrations of CO_2 and H_2O and due to increased residence time of the hot flue gases in the chamber. From the figure, the heating intensity was observed to be significantly higher in the first three sections during the PE two-staged combustion tests compared with other tests.

Summing up, the heat transfer ratio increases as oxygen concentration increases for all investigated combustion regimes and OEC methods, which complies with the results acquired with Horbaniuc et al. [10]. As a consequence, the heat transfer surfaces, e.g. process tubes in boilers, can be reduced if the boiler's heat output is required to be kept at the same level. As a consequence, the cost of process tubes is significantly reduced as well.

3.5. Combustion efficiency

Fig. 6 shows the variations of the combustion efficiency at different oxygen concentrations for the TEST B. The combustion efficiency can be defined as the ratio of the furnace heat flux (heat flux to the furnace wall or load) to the heat delivered with fuel. The heat delivered with the air and oxygen was not considered here. As shown in the figure, even minor O_2 enrichment results in rapid increase in combustion efficiency. That is one reason why low-level oxygen enrichment is commonly used in retrofit applications because incremental increase in efficiency is very significant.

The combustion efficiency of the combustion process was increased from 60% at 21% O_2 to 78% at 38% O_2 (or even to 82% at 46% O_2 when PE two-staged regime was used), i.e. more heat is available for the overall process. Additionally, increasing the oxygen concentration can in fact save energy, i.e. it can reduce fuel consumption when less fuel is required for a given unit of production because of the improvement in available heat.

4. Error analysis

The accuracy of the measurements was affected by the uncertainties arising from the accuracies of the used sensors (electrochemical sensors, thermocouples, flow meters). By applying the method of error propagation [21,22], the errors for NO_x and heat fluxes can be calculated.

As for the concentration of NO_x emission [mg/Nm^3], which was calculated based on the measured concentrations (in [ppm]) of NO and NO_2, the standard deviation of calculated NO_x holds the following equation Eq. (7):

$$\sigma_{NO_x} = \sqrt{\sigma_{NO}^2 + \sigma_{NO_2}^2} \tag{7}$$

The calculated relative errors are summarized in Table B.3 included in Appendix B. The highest errors (up to ±18%) were obtained for the AO tests in combination with gas staging for low levels of oxygen-enrichment. The reasons are that the uncertainty of NO_x is the combination of uncertainties of variables in the function and simultaneously the accuracy of NO and NO_2 sensors is ±5 ppm for low concentrations up to 99 ppm.

When the TEST B was carried out, the flow rate of cooling water through each section was reduced to its minimum which consequently improves the uncertainty of the heat flux measurement. The reason is that due to the lower flow rate of the cooling water the outlet temperature increases and hence the difference between the outlet and inlet temperature increases as well. Based on the calculation of propagation of uncertainty the heat flux measurement uncertainty is inversely proportional to the temperature difference. The standard deviation of calculated heat fluxes then holds Eq. (8):

$$\sigma_{\dot{q}_i} = \dot{q}_i \cdot \sqrt{\left[\left(\frac{\sigma_{V_i}}{V_i}\right)^2 + \frac{\sigma_{t_{OUT,i}}^2 + \sigma_{t_{IN}}^2}{\Delta t_i^2}\right]} \quad \text{for } i = 1, 2, \ldots, 7 \tag{8}$$

The calculated relative errors are summarized in Table B.4 in Appendix B. The maximum error was found to be within ±5% for the section 1 and ±3% for the sections 2–7.

5. Conclusions

In the present study, two types of combustion tests were carried out to investigate the effects of oxygen concentrations in the range of 21–46%. The influences of two oxygen-enhanced combustion methods and oxygen concentration on the NO_x emission, flue gas temperature, heat flux distribution, and flame characteristics were examined. The general conclusions drawn from the results of this work can be summed up as follows:

1. The NO_x emission increased sharply due to the higher furnace temperature as oxygen concentration increased during the PE tests. When the oxygen concentration was increased from 21% to 33%, the NO_x concentration increased more than by 40 times and by 20 times when one-staged and two-staged combustion regime was used, respectively. Significantly better results were obtained during the AO tests, especially when the fuel was staged. In this case the NO_x emission was below 120 mg/Nm^3 at all oxygen flow rates.
2. The radiative heat transfer was enhanced as oxygen concentration increased. The available heat at 33% O_2 was higher by approximately 20% compared with that at 21% O_2. At the same time the combustion efficiency increased from 61% to nearly 80%.
3. The produced oxygen-enhanced flames were stable and more luminous than the air/fuel flames. The increase of O_2 concentration caused that the OEC flame was longer by about 20% compared with air/fuel flame.

The future work of the research project will be focused on the investigation of the influence of another OEC method called as O_2 staging (also referred to as O_2 lancing) on the same combustion parameters like those studied in this work. Further, the temperature distribution in the middle plane of the combustion chamber will be measured for different oxygen enrichment levels and all studied OEC methods (premix enrichment, air-oxy/fuel, O_2 staging). Finally, the heating and furnace-temperature fixing tests will be carried out.

Acknowledgment

The authors gratefully acknowledge financial support provided within research projects No. P101/12/P747 “The influence of air enrichment with oxygen and oxygen injection into flame area on combustion process”, No. CZ.1.05/2.1.00/01.0002 “NETME center – new technologies for mechanical engineering”, and No. CZ.1.07/2.3.00/20.0020 “Science for practice”.

Appendix A

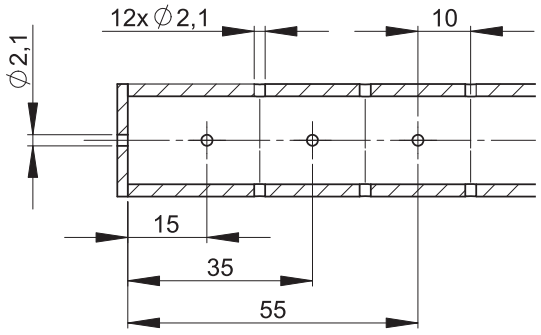

Fig. A.1. The schematic layout of the tip of the oxygen diffuser used for PE tests.

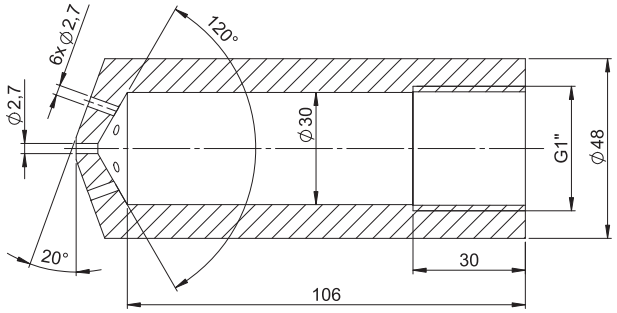

Fig. A.2. The schematic layout of the tip of the oxygen nozzle head used for AO tests.

Table A.1
The technical parameters of the sensors of the water cooling system.

Probe type	Sensor	Range	Accuracy ± 1digit
Temperature	Rawet PTP50J Pt100/B	(0–100) °C	±0.3% of measuring range
Flow rate	Sensus Type 420 S Qn 10	(0.15–40) m^3 h^{-1}	±0.5% of measured value

Table A.2
The technical parameters of the sensors of the flue gas analyzer.

Probe type	Range	Accuracy ± 1digit	Resolution
Thermocouple K	(−40 to 1200) °C	±0.5% of measured value	0.1 °C
O_2	(0–25) vol. %	±0.2 vol. %	0.01 vol. %
CO with H_2 compensation	(0–10000) ppm	• ±10 ppm in the range (0–199) ppm • ±5% of measured value in the range (200–2000) ppm	1 ppm
NO	(0–3000) ppm	• ±5 ppm in the range (0–99) ppm • ±5% of measured value in the range (100–2000) ppm	1 ppm
NO_2	(0–500) ppm	• ±5 ppm in the range (0–99) ppm • ±5% of measured value in the range (100–500) ppm	0.1 ppm
SO_2	(0–5000) ppm	• ±5 ppm in the range (0–99) ppm • ±5% of measured value in the range (0–2000) ppm	1 ppm

Appendix B

Table B.1
Data measured in TEST A.

Trial – combustion regime	O_2 flow rate [Nm^3/h]	Overall O_2 conc. [%]	NO (measured) [ppm]	NO_2 (measured) [ppm]	NO_x (calculated) [mg/Nm^3]	Flue gas temperature [°C]	Flame length [m]	Flame diameter [m]
PE one-staged	0	21.0	81.7	1.7	171	743	2.25	0.6
PE one-staged	5	21.5	92.7	2.0	195	755	2.25	0.6
PE one-staged	10	22.0	113.7	4.0	242	766	2.4	0.6
PE one-staged	20	23.1	180.0	5.7	381	761	2.5	0.6
PE one-staged	30	24.3	283.3	8.3	600	758	2.75	0.6
PE one-staged	40	25.6	524.7	14.3	1107	750	2.75	0.6
PE one-staged	60	29.0	1687.0	22.3	3511	743	3.1	0.6
PE one-staged	80	33.0	3410.0	46.0	7099	748	3.1	0.6
PE two-staged	0	21.0	36.0	4.0	82	699	2.3	1.0
PE two-staged	5	21.5	40.3	4.7	92	707	2.5	1.0
PE two-staged	10	22.0	46.3	5.0	105	708	2.5	1.0
PE two-staged	20	23.1	64.3	6.0	145	709	2.25	1.0
PE two-staged	30	24.3	90.	6.7	199	708	2.25	1.0
PE two-staged	40	25.6	145.7	8.3	316	705	2.5	1.0
PE two-staged	60	29.0	381.0	8.7	800	689	2.75	1.0
PE two-staged	80	33.0	822.3	17.0	1724	681	3.0	1.0
PE two-staged	100	38.0	1412.7	23.0	2949	665	3.0	1.0
PE two-staged	120	46.0	2383.0	43.7	4892	673	2.7	1.0
AO one-staged	0	21.0	81.7	1.7	171	743	2.25	0.6
AO one-staged	5	21.5	80.0	2.0	168	747	2.25	0.6
AO one-staged	10	22.0	86.3	2.0	181	758	2.25	0.6
AO one-staged	20	23.1	100.0	3.0	212	771	2.25	0.6
AO one-staged	30	24.3	130.0	4.0	275	781	2.5	0.6
AO one-staged	40	25.6	206.0	5.3	434	777	2.75	0.6
AO one-staged	60	29.0	564.7	10.3	1181	749	3.0	0.5
AO one-staged	80	33.0	754.3	14.3	1579	736	3.0	0.4
AO one-staged	100	38.0	694.0	11.7	1450	707	3.0	0.35
AO two-staged	0	21.0	36.0	4.0	82	699	2.3	1.0
AO two-staged	5	21.5	46.7	1.0	98	703	2.2	0.9
AO two-staged	10	22.0	43.7	1.0	92	704	2.2	0.9
AO two-staged	20	23.1	39.0	1.0	82	727	2.25	1.0
AO two-staged	30	24.3	39.3	1.7	84	708	2.5	1.0
AO two-staged	40	25.6	38.3	1.0	81	710	2.5	1.0
AO two-staged	60	29.0	49.7	1.0	104	676	2.4	0.9
AO two-staged	80	33.0	53.0	1.0	111	669	2.2	0.85
AO two-staged	100	38.0	40.3	1.0	85	651	2.2	0.85

Table B.2
Data measured in TEST B.

Trial – combustion regime	O_2 flow rate [Nm^3/h]	Overall O_2 conc. [%]	Heat flux							Heat transfer rate [kW]	Combustion efficiency [%]
			Section 1 [kW/m^2]	Section 2 [kW/m^2]	Section 3 [kW/m^2]	Section 4 [kW/m^2]	Section 5 [kW/m^2]	Section 6 [kW/m^2]	Section 7 [kW/m^2]		
PE one-staged	0	21.0	28.20	39.13	52.58	51.17	44.26	34.79	26.24	458.2	61.09
PE one-staged	40	25.6	31.88	46.21	59.23	57.27	48.99	37.11	26.82	506.7	67.09
PE one-staged	80	33.0	36.76	53.59	63.74	61.81	50.59	40.38	28.34	550.6	73.41
PE two-staged	0	21.0	28.64	51.96	60.80	48.57	39.73	30.77	23.50	466.6	62.20
PE two-staged	40	25.6	41.30	68.08	74.15	58.94	43.62	31.48	21.54	546.8	72.89
PE two-staged	80	33.0	43.78	71.54	82.68	62.94	44.96	31.29	22.99	580.1	77.59
PE two-staged	120	46.0	47.18	76.68	85.07	64.31	48.27	35.44	25.61	618.3	82.36
AO one-staged	0	21.0	28.20	39.13	52.58	51.17	44.26	34.79	26.24	458.2	61.09
AO one-staged	40	25.6	28.73	42.53	57.16	58.96	50.82	38.75	28.37	506.2	67.41
AO one-staged	80	33.0	38.51	50.45	63.72	64.50	57.68	44.84	30.60	576.6	76.84
AO two-staged	0	21.0	28.64	51.96	60.80	48.57	39.73	30.77	23.50	466.6	62.20
AO two-staged	40	25.6	37.66	56.51	62.79	56.46	46.81	35.88	26.35	527.8	70.30
AO two-staged	80	33.0	46.03	62.49	69.02	62.74	52.73	41.16	27.25	587.5	78.12

Table B.3
Error analysis of NO_x.

Trial – combustion regime	Flow rate of O_2 [Nm^3/h]	Overall O_2 concentration [%]	NO_x (calculated) [mg/Nm^3]	Relative error [%]
PE one-staged	0	21.0	171	8.5
PE one-staged	5	21.5	195	7.5
PE one-staged	10	22.0	242	6.4
PE one-staged	20	23.1	381	5.5
PE one-staged	30	24.3	600	5.1
PE one-staged	40	25.6	1107	5.0
PE one-staged	60	29.0	3511	4.9
PE one-staged	80	33.0	7099	4.9
PE two-staged	0	21.0	82	17.7
PE two-staged	5	21.5	92	15.7
PE two-staged	10	22.0	105	13.8
PE two-staged	20	23.1	145	10.0
PE two-staged	30	24.3	199	7.3
PE two-staged	40	25.6	316	5.7
PE two-staged	60	29.0	800	5.1
PE two-staged	80	33.0	1724	4.9
PE two-staged	100	38.0	2949	4.9
PE two-staged	120	46.0	4892	4.9
AO one-staged	0	21.0	171	8.5
AO one-staged	5	21.5	168	8.6
AO one-staged	10	22.0	181	8.0
AO one-staged	20	23.1	212	6.9
AO one-staged	30	24.3	275	6.1
AO one-staged	40	25.6	434	5.4
AO one-staged	60	29.0	1181	5.0
AO one-staged	80	33.0	1579	4.9
AO one-staged	100	38.0	1450	5.0
AO two-staged	0	21.0	82	17.7
AO two-staged	5	21.5	98	14.8
AO two-staged	10	22.0	92	15.8
AO two-staged	20	23.1	82	17.7
AO two-staged	30	24.3	84	17.2
AO two-staged	40	25.6	81	18.0
AO two-staged	60	29.0	104	13.9
AO two-staged	80	33.0	111	13.1
AO two-staged	100	38.0	85	17.1

Table B.4
Error analysis of heat fluxes.

Trial – combustion regime	O_2 flow [Nm^3/h]	Overall O_2 conc. [%]	Relative error						
			Section 1 [%]	Section 2 [%]	Section 3 [%]	Section 4 [%]	Section 5 [%]	Section 6 [%]	Section 7 [%]
PE one-staged	0	21.0	4.7	2.6	1.7	2.0	2.2	2.7	2.0
PE one-staged	40	25.6	4.1	2.2	1.5	1.8	2.0	2.4	2.0
PE one-staged	80	33.0	3.0	1.7	1.3	1.6	1.6	2.1	2.0
PE two-staged	0	21.0	3.5	1.6	1.3	1.9	1.9	2.3	2.1
PE two-staged	40	25.6	2.9	1.4	1.3	1.7	2.1	2.7	2.6
PE two-staged	80	33.0	2.6	1.3	1.1	1.6	2.1	2.3	2.6
PE two-staged	120	46.0	2.6	1.3	1.2	1.6	2.0	2.4	2.1
AO one-staged	0	21.0	4.7	2.6	1.7	2.0	2.2	2.7	2.0
AO one-staged	40	25.6	4.1	2.1	1.5	1.7	1.9	2.0	1.9
AO one-staged		33.0	3.0	1.7	1.4	1.5	1.6	1.7	1.7
AO two-staged	0	21.0	3.5	1.6	1.3	1.9	1.9	2.3	2.1
AO two-staged	40	25.6	3.1	1.5	1.4	1.7	2.0	2.1	2.0
AO two-staged	80	33.0	2.5	1.6	1.3	1.6	1.7	2.2	2.0

References

[1] Baukal CE. Industrial burners handbook. Boca Raton, USA: CRC Press LLC; 2004.
[2] Baukal CE. Oxygen-enhanced combustion. Boca Raton, USA: CRC Press LLC; 1998.
[3] Mondal MK, Balsora HK, Varchney P. Progress and trends in CO_2 capture/separation technologies: a review. Energy 2012;46:431–41.
[4] Wall TF. Combustion processes for carbon capture. Proc Combust Inst 2007;31:31–47.
[5] Gronkvist S, Bryngelsson M, Westermark M. Oxygen efficiency with regard to carbon capture. Energy 2006;31:3220–6.
[6] Wu KK, Chang YC, Chen CH, Chen YD. High-efficiency combustion of natural gas with 21–30% oxygen-enriched air. Fuel 2010;89:2455–62.
[7] Merlo N, Boushaki T, Chauveau Ch, Persis SD, Pillier L, Sarh B, Gokalp I. Combustion characteristics of methane-oxygen enhanced air turbulent non-premixed swirling flames. Exp Therm Fluid Sci; 2013.
[8] Daood SS, Nimmo W, Edge P, Gibbs BM. Deep-staged, oxygen enriched combustion of coal. Fuel 2012;101:187–96.
[9] Tan Y, Douglas MA, Thambimuthu KV. CO_2 capture using oxygen enhanced combustion strategies for natural gas power plants. Fuel 2002;81:1007–16.
[10] Horbaniuc B, Marin O, Domitraşcu G, Charon O. Oxygen-enriched combustion in supercritical steam boilers. Energy 2004;29:427–48.
[11] Qiu K, Hayden ACS. Increasing the efficiency of radiant burners by using polymer membranes. Appl Energy 2009;86:349–54.
[12] Lambert J, Sorin M, Paris J. Analysis of oxygen-enriched combustion for steam methane reforming (SMR). Energy 1997;22:817–25.
[13] Sánchez M, Cadavid F, Amell A. Experimental evaluation of a 20 kW oxygen enhanced self-regenerative burner operated in flameless combustion mode. Appl Energy 2013;111:240–6.
[14] Bělohradský P, Kermes V. Experimental study on NO_x formation in gas-staged burner based on the design of experiments. Chem Eng Trans 2012;29:79–84.
[15] Kermes V, Bělohradský P. Biodiesel (EN 14213) heating oil substitution potential for petroleum based light heating oil in a 1 MW stationary combustion facility. Biomass Bioenergy 2013;49:10–21.
[16] Baukal CE. Industrial combustion pollution and control. New York, USA: Marcel Dekker; 2004.
[17] Persis S, Foucher F, Pillier L, Osorio V, Gökalp I. Effects of O_2 enrichment and CO_2 dilution on laminar methane flames. Energy 2013;55:1055–66.
[18] Abdelaal MM, Rabee BA, Hegab AH. Effect of adding oxygen to the intake air on a dual-fuel engine performance, emissions, and knock tendency. Energy 2013;6:612–20.
[19] Souza GR, Santos AM, Ferreira AL, Martins KCR, Módolo DL. Evaluation of the performance of biodiesel from waste vegetable oil in a flame tube furnace. Appl Therm Eng 2009;29:2562–6.
[20] Bašta J. Heat transfer surfaces. Prague, Czech Republic: ČVUT; 2001 [in Czech].
[21] Braembussche VD. Measurement techniques in fluid dynamics: an introduction. Rhode Saint Genése: von Karman Institute for Fluid Dynamics; 2001.
[22] Bevington P, Robinson DK. Data reduction and error analysis for the physical sciences. New York, USA: McGraw-Hill; 2002.